CHIN. PHYS. LETT. Vol. 38, No. 6 (2021) 063201

Coherent Control of High Harmonic Generation Driven by Metal Nanotip Photoemission

Hongdan Zhang(张宏丹)[1,2], Xiwang Liu(刘希望)[1,2], Facheng Jin(金发成)[1,2,4], Ming Zhu(朱明)[1], Shidong Yang(杨士栋)[1,2], Wenhui Dong(董文卉)[1], Xiaohong Song(宋晓红)[1,2,3*], and Weifeng Yang(杨玮枫)[1,2,3*]

[1]*Research Center for Advanced Optics and Photoelectronics, Department of Physics, College of Science, Shantou University, Shantou 515063, China*
[2]*Institute of Mathematics, Shantou University, Shantou 515063, China*
[3]*Key Laboratory of Intelligent Manufacturing Technology of MOE, Shantou University, Shantou 515063, China*
[4]*Faculty of Science, Xi'an Aeronautical University, Xi'an 710077, China*

(Received 21 January 2021; accepted 20 April 2021; published online 25 May 2021)

Steering ultrafast electron dynamics with well-controlled laser fields is very important for generation of intense supercontinuum radiation. It can be achieved through coherent control of the symmetry of the interaction between strong-field laser fields and a metal nanotip. We employ a scheme of two-color laser pulses combined with a weak static field to realize the control of a single quantum path to generate high harmonic generation from a single solid-state nanoemitter. Moreover, a smooth and ultrabroad supercontinuum in the extreme ultraviolet region is obtained, which can produce a single attosecond pulse. Our findings are beneficial for efficient generation of isolated sub-100 as XUV pulses from solid-state sources.

DOI: 10.1088/0256-307X/38/6/063201

Manipulating ultrafast electronic dynamics on the (sub)femtosecond time is at the heart of strong-field physics and attosecond science.[1−20] High-order harmonic generation (HHG) from atoms or molecules is one of the most fundamental processes in strong-field attosecond physics. The physics of HHG has been well described in a three-step model[21] as follows: an electron first tunnels through the barrier created by the Coulomb potential and the laser electric fields; it is subsequently accelerated by the laser fields; finally, it is pulled back by the laser fields and recombined with the parent ion, which emits high-energy extreme-ultraviolet radiation, i.e., attosecond pulse train or isolated attosecond pulse.[3,4,22−25] The HHG spectra along with the photoelectron spectra provide efficient tools for extracting the information of the electronic and structural dynamics with both subfemtosecond temporal and subangstrom spatial resolution.[26−30]

Over the past decade, the interaction between strong laser fields and solid-state media has garnered significant attention.[31−39] For example, instead of employing atoms and molecules in the gas phase, HHG from bulk matter has been demonstrated in experiments.[31] A generalized three-step model has been proposed to provide an intuitive picture of inter-band HHG in solids similar to atomic HHG.[32]

Metallic nanostructures with appropriate geometries can lead to the nanofocusing of the propagating surface plasmon polariton waves beyond the diffraction limit and create a strong and spatially isolated nanometer-sized light source. Owing to the near-field enhancement effect, the incoming laser field from a laser oscillator can be locally amplified to enter the strong-field regime. By injecting noble gases into the nanostructures, HHG can be obtained with a high repetition rate.[40] Experimental demonstrations of plasmonic field-enhanced HHG have been performed using both gold bow-tie-shaped nanostructures and cone-shaped funnel waveguides.[41,42]

Recently, it has been experimentally demonstrated that photoelectrons emitted directly from the metal nanotips can also re-collide with the metal surface, resulting in high-energy electrons. The overall shape of the photoelectron spectra, including the re-scattering plateau and its cutoff, is very similar to that of the atomic cases. Moreover, it has been demonstrated that the three-step model in atomic physics can still be applied to explain the spectra, which paves the way for the extension of attosecond physics from atoms, molecules to solid nanoemitters.[43,44] The main phys-

Supported by the National Key Research and Development Program of China (Grant Nos. 2019YFA0307700 and 2016YFA0401100), the National Natural Science Foundation of China (Grant Nos. 11774215, 11674209, 91950101, 11947243, 11334009, 11425414, and 11947080), Sino-German Mobility Programme (Grant No. M-0031), Department of Education of Guangdong Province (Grant No. 2018KCXTD011), High Level University Projects of the Guangdong Province (Mathematics, Shantou University), and the Open Fund of the State Key Laboratory of High Field Laser Physics (SIOM).
*Corresponding author. Email: songxh@stu.edu.cn; wfyang@stu.edu.cn
© 2021 Chinese Physical Society and IOP Publishing Ltd

ical mechanism behind the HHG is the electron recollision, which has been demonstrated in metal nanotips. Moreover, weak high harmonics beyond the third harmonic order from a metal surface have been observed experimentally, and HHG from metal nanotips has been put forth.[45] With a fully quantum mechanical model, Ciappina *et al.*[46] have shown that use of metal tips as an active medium should provide an alternative way to generate coherent XUV light using a femtosecond laser field. Moreover, they observed a strong modulation of HHG spectra with a varying carrier-envelope phase for short pulses. The HHG cutoff has been extended along with an increase in the harmonic yield when positive static fields are employed. However, as stated by the authors, a more comprehensive investigation of the effect of the static fields arising owing to the dc metal tip bias voltage in the HHG spectra is necessary.

In this Letter, an efficient method has been proposed for generation of isolated broadband attosecond pulses using two-color midinfrared laser fields in combination with a static field to drive metal nanotips. Compared with atomic gases, metal nanotips are more likely to generate isolated attosecond pulses. The subcycle attosecond pules with a duration of 74 as can be generated by choosing an appropriate relative phase of the two-color pulse, and with the help of a static field. Atomic units (a.u.) are employed throughout this paper unless otherwise stated.

The theoretical model we employed is the same as that in Ref. [46], which has been successfully chosen for modeling the rescattering induced high energy photoemission from metal nanotips and corresponds with the experimental data. It is based on the numerical integration of the time-dependent Schrödinger equation (TDSE) as follows:

$$i\frac{\partial\Psi(z,t)}{\partial t} = \Big[-\frac{1}{2}\frac{\partial^2}{\partial z^2} + V_m(z) + V_l(z,t)\Big]\Psi(z,t), \quad (1)$$

where $V_m(z)$ denotes the potential of the nanotip and $V_l(z,t) = [E_l(t) + E_{\rm dc}]z$ the interaction potential due to the oscillating electric field $E_l(t)$ and the applied static field $E_{\rm dc}$. A narrow semi-infinite potential well is used to describe the metal-vacuum interface. On the side of the nanotip, the electron wave function is confined by an infinitely high potential wall, and on the other side by a potential step representing the metal-vacuum surface barrier. The depth of the well inside the metal ($z \le 0$) is described by $V_m(z) = -(W + E_F)$, where $W = 5.5\,{\rm eV}$ denotes the work function and $E_F = 4.5\,{\rm eV}$ the Fermi energy for clean gold.[46] The image-force potential is considered, which gives a smoother shape to the surface barrier potential. The potential well ($z \ge 0$) can be expressed as $V_m(z) = -1/(z+\alpha)$ with $\alpha = 1.4\,{\rm a.u.}$ to make $V_m(z)$ continuous at $z = 0$. In our simulation, we used this model to study single sub-cycle ultrashort attosecond generation in two-color midinfrared laser fields. The synthesized two-color midinfrared laser field is expressed as follows:

$$\begin{aligned} E_l(t) = {} & E_1 \exp[-2(\ln 2)t^2/\tau_1^2]\cos(\omega_1 t) \\ & + E_2 \exp[-2(\ln 2)t^2/\tau_2^2]\cos(\omega_2 t + \Delta\phi). \end{aligned} \quad (2)$$

Here, E_1 and E_2 are the electric-field amplitudes of the fundamental pulse(ω_1) and the one half frequency(ω_2), respectively; τ_1 and τ_2 denote the full widths at half maximum of two laser fields, respectively. $\Delta\phi$ denotes the relative phase between the two pulses.

In this study, the ground state is selected as the initial state of the metal nanotip, and it is calculated using the imaginary-time evolutionary algorithm without $V_l(z,t)$ in the Schrödinger equation. Furthermore, the time-dependent wave function of the electron is obtained by solving the one-dimensional TDSE using the split-operator method. Ideally, as we know, the wave function decays to zero at infinity, but the space is limited in the calculation. Hence, the box boundary is set as $z_{\rm max} = 450\,{\rm a.u.}$, which is located sufficiently far away from the core region. Furthermore, a mask function[47] is selected to avoid spurious effects and reflections near the box edges, which is expressed as follows:

$$M(z_b) = \Big[1 + \exp\Big(\frac{|z| - z_b}{\delta}\Big)\Big]^{-1}, \quad (3)$$

where the absorbing boundary $z_b = 300\,{\rm a.u.}$, and the decay factor $\delta = 6\,{\rm a.u.}$ is selected in this simulation. Fourier transforming the dipole acceleration $a(t)$, we can retrieve the harmonic spectra $D(\omega)$ as follows:

$$D(\omega) = \Big|\frac{1}{T_{\rm p}}\frac{1}{\omega^2}\int_{-\infty}^{\infty} {\rm e}^{-i\omega t} a(t)dt\Big|^2, \quad (4)$$

where $T_{\rm p}$ is the total duration of the laser pulse. The expectation value of the dipole acceleration is calculated as follows:

$$a(t) = -\Big\langle\Psi(z,t)\Big|\frac{\partial V(z,t)}{\partial z}\Big|\Psi(z,t)\Big\rangle, \quad (5)$$

where $V(z,t) = V_m(z)$. To obtain the detailed information within HHG, the time-frequency spectrum can be obtained by the wavelet transform[48,49]

$$A_w(t_0,\omega) = \int a(t) w_{t_0,\omega}(t)dt, \quad (6)$$

where the wavelet kernel is $w_{t_0,\omega}(t) = \sqrt{\omega}W[\omega(t-t_0)]$, and the Morlet wavelet $W(x) = (1/\sqrt{\tau}){\rm e}^{\rm ix}{\rm e}^{-x^2/2\tau^2}$ is chosen for harmonic emission. Finally, the attosecond pulse can be further obtained by superposing several harmonics (with q the harmonic order):

$$I(t) = \Big|\sum_q a_q e^{iq\omega t}\Big|^2, \quad (7)$$

with $a_q = \int a(t)e^{-iq\omega t}dt$.

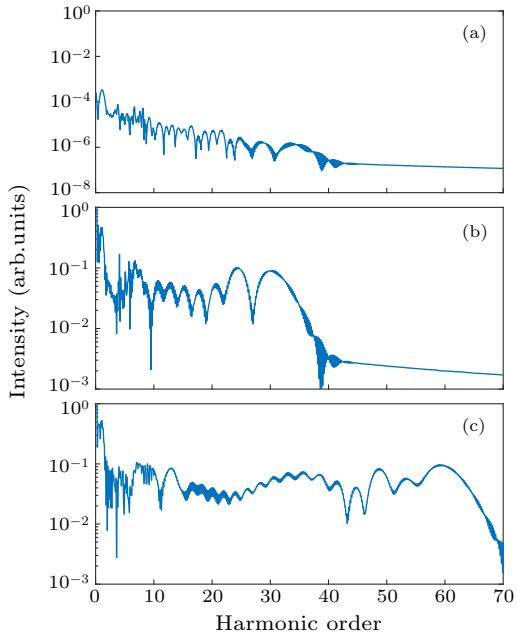

Fig. 1. HHG spectra of (a) atom and (b) metal nanotip driven by a single laser pulse with wavelength $\lambda_1 = 1350\,\text{nm}$, and intensity $I_1 = 40 \times 10^{12}\ \text{W/cm}^2$. (c) HHG spectrum from metal nanotip by adding another field with $\lambda_2 = 2700\,\text{nm}$, $I_2 = 4 \times 10^{12}\ \text{W/cm}^2$ and $\Delta\phi = 0$ to the driving field.

To compare the efficiency of producing HHG between gas atoms and metal nanotips, we perform a quantum simulation to obtain the HHG spectrum of atoms by solving the TDSE. We choose the soft-core model within the single-active-electron approximation $V(z) = -1/\sqrt{\alpha + z^2}$, which has been employed in several studies of atomic ionization and HHG. Here smoothing parameter $\alpha = 7\,\text{a.u.}$ guarantees the same ionization energy of the atom and the nanotip. Figure 1(a) shows the harmonic spectrum of an atom driven by a single laser pulse with wavelength $\lambda_1 = 1350\,\text{nm}$ and intensity $I_1 = 40 \times 10^{12}\ \text{W/cm}^2$, which lasts for ten optical cycles. In contrast to Fig. 1(a), the harmonic spectrum of metal nanotips driven by the same pulse in Fig. 1(b) shows a higher harmonic intensity and clearer platform structure, which would significantly benefit the production of isolated attosecond pulse. For symmetric gas atoms, the attosecond pulses emit once every half-cycle with comparable intensity, with modulations presented in HHG. For an asymmetric metal nanotip, the attosecond pulses emit once within one optical cycle due to the symmetry breaking of Coulomb potential. By adding another field with wavelength $\lambda_2 = 2700\,\text{nm}$, intensity $I_1 = 4 \times 10^{12}\ \text{W/cm}^2$ and $\Delta\phi = 0$ to the driving field, the electron dynamics can be modulated. The electrons which generate the harmonics near the cutoff region would gain much higher kinetic energy before returning to the parent ion. Thus, the harmonic cutoff can be extended, as shown in Fig. 1(c). One can clearly observe that harmonics in the low energy region are chaotic, which originates from the interference of different quantum trajectories. The trajectory of the electron with a later ionization time but an earlier recombination time is called the short trajectory. The trajectory of the electron with an earlier ionization time but a later recombination time is called the long trajectory.[50,51]

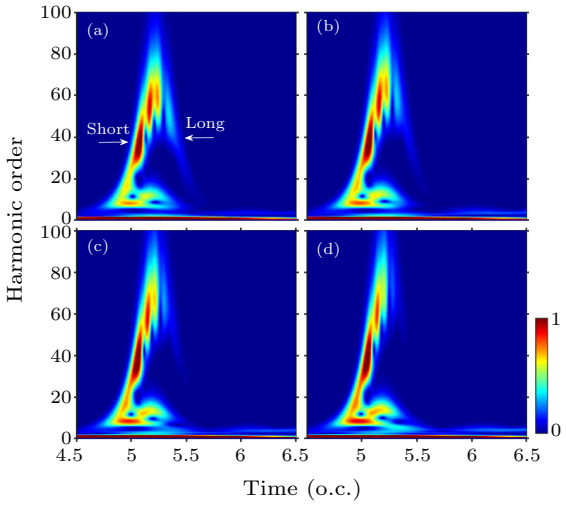

Fig. 2. Time-frequency spectra (a)–(d) in the synthesized field with different intensities of static field 0, 0.001, 0.002, and 0.003, respectively. Time is in units of optical cycle (o.c.).

To generate an isolated attosecond pulse, single quantum trajectory control must be realized. It has been demonstrated that the long and short trajectories can be significantly controlled through the static field.[52,53] Hence, we can consider the selection of the electron trajectories by adding a static field to the two-color driving field. We further vary E_{dc} from 0 to 0.003 a.u. to study the time-frequency spectra in the synthesized field. As shown in Fig. 2, the effect of the static field on selection of electron trajectories becomes increasingly clear as the intensity of E_{dc} increases; the corresponding intensity values of Figs. 2(a)–2(d) are approximately 0, 0.001, 0.002, and 0.003 a.u. in our calculations. It can be seen more clearly that the contribution of long trajectory is gradually suppressed as the intensity of electrostatic field increases, which implies that a single quantum path contributing to the continuous harmonic generation is selected. The interference between the short and long trajectories will be weak with single quantum trajectory control. Thus, the modulation will also be weak and a supercontinuum of the harmonic spectrum can be obtained.

In the following, we investigate the harmonic spectrum in the synthesized field with different relative phases $\Delta\phi$ between the control and fundamental fields. The harmonic spectrum for different relative

phases from $-\pi$ to π are shown in Fig. 3(a). One can clearly see that smooth supercontinuum is generated in the plateau region for all the relative phases. To obtain an attosecond pulse as short as possible, a sufficiently wide supercontinuum spectrum must be guaranteed. Notably, the widest supercontinuum occurs when the relative phase $\Delta\phi = 0$, as shown in Fig. 4(a). In order to explain the physical origin of the supercontinuum, the time-frequency spectra have been shown for $\Delta\phi = 0.5\pi$, 0 and -0.5π, respectively. For $\Delta\phi = 0.5\pi$ and -0.5π [Figs. 3(b) and 3(d)], it can be seen that the long and short trajectories make contributions to the HHG, which induces the interference structure in HHG. For $\Delta\phi = 0$ [Fig. 3(c)], it is found that the long trajectory has been deeply depressed, while the HHG mainly comes from the contribution of the short trajectory, which leads to the formation of the widest supercontinuum.

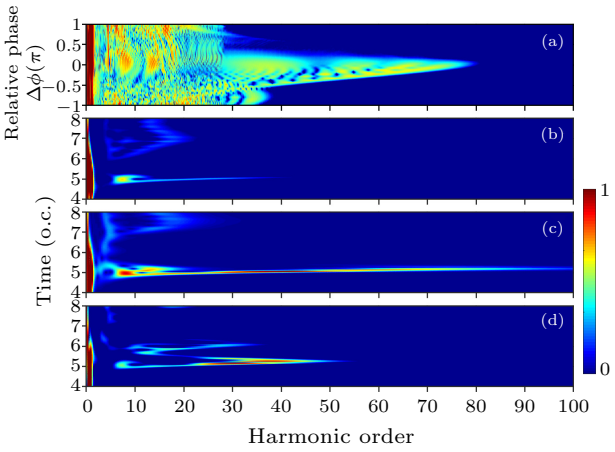

Fig. 3. (a) Harmonic spectrum as a function of relative phases $\Delta\phi$ from $-\pi$ to π. Time-frequency spectra for (b) $\Delta\phi = 0.5\pi$, (c) $\Delta\phi = 0$ and (d) $\Delta\phi = -0.5\pi$.

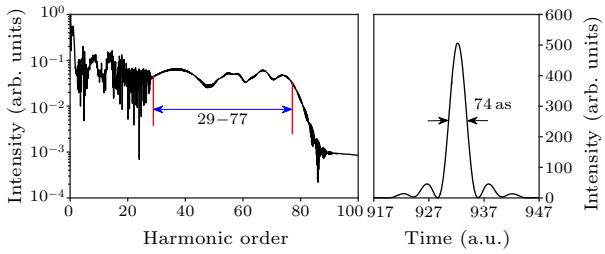

Fig. 4. (a) Harmonic spectrum for relative phase $\Delta\phi = 0$. (b) Temporal profiles of the generated isolated attosecond pulses synthesized by the supercontinuum shown in (a), with time in atomic units.

Figure 4(b) shows the temporal profiles of the attosecond pulses generated in the synthesized driving field by superposing the harmonics from 29 ω_1 to 77 ω_1, single attosecond pulses with duration 74 as can be obtained in the Fourier-transform limit for the above cases. The isolated 74 as the pulse provides us with the potential resolving more ultrafast electronic dynamics in the microworld. Moreover, owing to the high photon energy, one can gain more insight into inner-shell electrons dynamics.

In conclusion, we have proposed an efficient method to generate an isolated attosecond pulse from sharp metal nanotips, using a two-color driving pulse in combination with a static field. Compared to atoms, the asymmetric metal nanotip provides a promising source to generate a supercontinuum spectrum and further produce attosecond pulses. It is shown that the electron would gain a much higher kinetic energy in the two-color field before returning to its parent ion. Hence, the harmonic cutoff can be extended effectively. In addition, the single quantum trajectory control can be realized by adding the static field to the two-color field. An isolated attosecond pulse with duration of 74 as can be obtained.

References

[1] Krausz F and Ivanov M 2009 *Rev. Mod. Phys.* **81** 163
[2] Corkum P B and Krausz F 2007 *Nat. Phys.* **3** 381
[3] Salières P, Carré B, Le D L, Grasbon F, Paulus G G, Walther H, Kopold R, Becker W, Milošević D B, Sanpera A and Lewenstein M 2001 *Science* **292** 902
[4] Mairesse Y, de B A, Frasinski L J, Merdji H, Dinu L C, Monchicourt P, Breger P, Kovačev M, Taïeb R, Carré B, Muller H G, Agostini P and Salières P 2003 *Science* **302** 1540
[5] Song X H, Gong S Q, Yang W F, Jin S Q, Feng X L and Xu Z Z 2004 *Opt. Commun.* **236** 151
[6] Yang W F, Song X H, Gong S Q, Cheng Y and Xu Z Z 2007 *Phys. Rev. Lett.* **99** 133602
[7] Liu X W, Zhang G J, Li J, Shi G L, Zhou M Y, Huang B Q, Tang Y J, Song X H and Yang W F 2020 *Phys. Rev. Lett.* **124** 113202
[8] Li F, Yang Y J, Chen J, Liu X J, Wei Z Y and Wang B B 2020 *Chin. Phys. Lett.* **37** 113201
[9] Gong X C, Lin C, He F, Song Q Y, Lin K, Ji Q Y, Zhang W B, Ma J Y, Lu P F, Liu Y Q, Zeng H P, Yang W F and Wu J 2017 *Phys. Rev. Lett.* **118** 143203
[10] Song X H, Shi G L, Zhang G J, Xu J W, Lin C, Chen J and Yang W F 2018 *Phys. Rev. Lett.* **121** 103201
[11] Song X H, Xu J W, Lin C, Sheng Z H, Liu P, Yu X H, Zhang H T, Yang W F, Hu S L, Chen J, Xu S P, Chen Y J, Quan W and Liu X J 2017 *Phys. Rev. A* **95** 033426
[12] Sun T, Zhang S W, Wang R, Feng S, Liu Y, Lv H and Xu H F 2020 *Chin. Phys. Lett.* **37** 043301
[13] Yang W F, Zhang H T, Lin C, Xu J W, Sheng Z H, Song X H, Hu S L and Chen J 2016 *Phys. Rev. A* **94** 043419
[14] Song X H, Hao Z Z, Yan M, Wu M L and Yang W F 2015 *Laser Phys. Lett.* **12** 105003
[15] Chen Z J, Zheng Y Y, Yang W F, Song X H, Xu J L, Dimauro L F, Zatsarinny O, Bartschat K, Morishita T, Zhao S F and Lin C D 2015 *Phys. Rev. A* **92** 063427
[16] Yang W F, Sheng Z H, Feng X P, Wu M L, Chen Z J and Song X H 2014 *Opt. Express* **22** 2519
[17] Wang X W, Wang L, Xiao F, Zhang D W, Lv Z H, Yuan J M and Zhao Z X 2020 *Chin. Phys. Lett.* **37** 023201
[18] Yang W F, Song X H, Zeng Z N, Li R X and Xu Z Z 2010 *Opt. Express* **18** 2558
[19] Zhang J, Hua L Q, Chen Z, Zhu M F, Gong C and Liu X J 2020 *Chin. Phys. Lett.* **37** 124203
[20] Zhang C J, Yang W F, Song X H and Xu Z Z 2009 *Phys. Rev. A* **79** 043823
[21] Corkum P B 1993 *Phys. Rev. Lett.* **71** 1994

[22] Sansone G, Benedetti E, Calegari F, Vozzi C, Avaldi L, Flammini R, Poletto L, Villoresi P, Altucci C, Velotta R, Stagira S, Silvestri S D and Nisoli M 2006 *Science* **314** 443
[23] Song X H, Gong S Q, Yang W F and Xu Z Z 2004 *Phys. Rev. A* **70** 013817
[24] Yang W F, Gong S Q, Li R X and Xu Z Z 2007 *Phys. Lett. A* **362** 37
[25] Mashiko H, Gilbertson S, Li C, Khan S D, Shakya M M, Moon E and Chang Z 2008 *Phys. Rev. Lett.* **100** 103906
[26] Baker S, Robinson J S, Haworth C A, Teng H, Smith R A, Chirila C C, Lein M, Tisch J G and Marangos J P 2006 *Science* **312** 424
[27] Haessler S, Caillat J, Boutu W, Giovanetti-Teixeira C, Ruchon T, Auguste T, Diveki Z, Breger P, Maquet A, Carré B, Taïeb R and Salières P 2010 *Nat. Phys.* **6** 200
[28] Smirnova O, Mairesse Y, Patchkovskii S, Dudovich N, Villeneuve D, Corkum P and Ivanov M Y 2009 *Proc. Natl. Acad. Sci. USA* **106** 16556
[29] Smirnova O, Mairesse Y, Patchkovskii S, Dudovich N, Villeneuve D, Corkum P B and Ivanov M Y 2009 *Nature* **460** 972
[30] Power E P, March A M, Catoire F, Sistrun E, Krushelnick K, Agostini P and DiMauro L F 2010 *Nat. Photon.* **4** 352
[31] Ghimire S, DiChiara A D, Sistrunk E, Agostini P, DiMauro L F and Reis D A 2011 *Nat. Phys.* **7** 138
[32] Vampa G, McDonald C R, Orlando G, Klug D D, Corkum P B and Brabec T 2014 *Phys. Rev. Lett.* **113** 073901
[33] Fu S L, Feng Y K, Li J B, Yue S J, Zhang X, Hu B T and Du H C 2020 *Phys. Rev. A* **101** 023402
[34] Song X H, Yang S D, Zuo R X, Meier T and Yang W F 2020 *Phys. Rev. A* **101** 033410
[35] Jiang S C, Chen J G, Wei H, Yu C, Lu R F and Lin C D 2018 *Phys. Rev. Lett.* **120** 253201
[36] Song X H, Zuo R X, Yang S D, Li P C, Meier T and Yang W F 2019 *Opt. Express* **27** 2225
[37] Li L, Lan P F, Zhu X S, Huang T F, Zhang Q B, Lein M and Lu P X 2019 *Phys. Rev. Lett.* **122** 193901
[38] Zuo R X, Song X H, Liu X W, Yang S D and Yang W F 2019 *Chin. Phys. B* **28** 094208
[39] Song X H, Wang N N, Yan M, Lin C, Förstner J, Yang W F 2017 *Opt. Express* **25** 13207
[40] Kim S, Jin J, Kim Y, Park I, Kim Y and Kim S 2008 *Nature* **453** 757
[41] Han S, Kim H, Kim Y W, Kim Y J, Kim S C, Park I Y and Kim S 2016 *Nat. Commun.* **7** 13105
[42] Sivis M, Duwe M, Abel B and Ropers C 2013 *Nat. Phys.* **9** 304
[43] Krüger M, Schenk M and Hommelhoff P 2011 *Nature* **475** 78
[44] Förster M, Paschen T, Krüger M, Lemell C, Wachter G, Libisch F, Madlener T, Burgdörfer J and Hommelhoff P 2016 *Phys. Rev. Lett.* **117** 217601
[45] Krüger M, Schenk M, Förster M and Hommelhoff P 2012 *J. Phys. B* **45** 074006
[46] Ciappina M F, Pérez-Hernández J A, Shaaran T, Lewenstein M, Krüger M and Hommelhoff P 2014 *Phys. Rev. A* **89** 013409
[47] Heather R and Metiu H 1987 *J. Chem. Phys.* **86** 5009
[48] Antoine P, Piraux B and Maquet A 1995 *Phys. Rev. A* **51** R1750
[49] Tong X M and Chu S I 2000 *Phys. Rev. A* **61** 021802
[50] Lewenstein M, Salières P and L'Huillier A 1995 *Phys. Rev. A* **52** 4747
[51] Bellini M, Lyngå C, Tozzi A, Gaarde M B, Hänsch T W, L'Huillier A and Wahlström C G 1998 *Phys. Rev. Lett.* **81** 297
[52] Serrat C and Biegert J 2010 *Phys. Rev. Lett.* **104** 073901
[53] Xia C L, Zhang G T, Wu J and Liu X S 2010 *Phys. Rev. A* **81** 043420